ACS APPLIED MATERIALS & INTERFACES

LETTER

www.acsami.org

Carbon Microspheres as Ball Bearings in Aqueous-Based Lubrication

J. E. St.Dennis, Kejia Jin, Vijay T. John, and Noshir S. Pesika*

Department of Chemical and Biomolecular Engineering, Tulane University, 6823 St. Charles Avenue, New Orleans, Louisiana 70118, United States

Supporting Information

ABSTRACT: We present an exploratory study on a suspension of uniform carbon microspheres as a new class of aqueous-based lubricants. The surfactant-functionalized carbon microspheres (~0.1 wt %) employ a rolling mechanism similar to ball bearings to provide low friction coefficients ($\mu \approx 0.03$) and minimize surface wear in shear experiments between various surfaces, even at high loads and high contact pressures. The size range, high monodispersity, and large yield stress of the $C_{\mu sphere}$, as well as the minimal environmental impact, are all desirable characteristics for the use of a $C_{\mu sphere}$-SDS suspension as an alternative to oil-based lubricants in compatible devices and machinery.

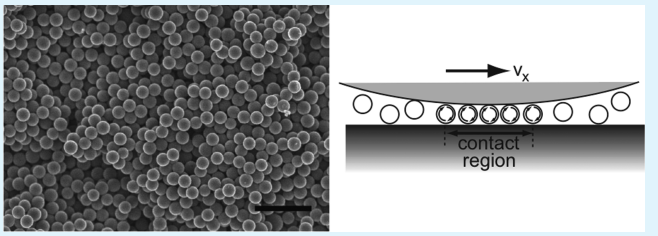

KEYWORDS: friction, lubrication, ball bearings, wear, microspheres

The history of tribology can be traced back to 1880 BC in Egypt, where lubricants (water and oil) were used to reduce friction between the sleigh, which supported a 60-ton statue, and the boards upon which it slid.[1] Today, lubricants play an integral role in the operation of several technologies, including internal combustion engines, vehicles, gear systems, compressors, turbines, and hydraulics in addition to smaller scale technologies, including the lubrication of hard disk drives[2] and microelectromechanical systems (MEMs).[3] The main functions of a lubricant are to reduce friction and material wear.

Typical boundary lubricants (also referred to as thin film lubrication) are composed of 93% base oils and 7% additives, and there are approximately 5000−10 000 different lubricant formulations, each for a specific application.[4] The additives serve several purposes including viscosity index improvers (which allow the lubricant to attain desired viscosities at particular temperatures), antioxidant agents, anticorrosion agents, wear-protection agents, acid neutralizers, antimicrobials, and dispersants. The environmental impact, degradation and health hazards of lubricants are still concerns, which have yet to be fully quantified.[5,6]

Another class of lubricants makes use of ball bearings that employ a "rolling" mechanism to reduce friction between sliding surfaces. The concept of using nanometer-sized spherical particles as nanoball bearings is not novel. Several studies in the early 1990s[7−13] looked into the possibility of using C_{60} (or bucky balls) as additives to oil-based lubricants. C_{60} molecules have a diameter of approximately 1 nm and a low volume compressibility (7×10^{-12} cm^2 dyn^{-1}), which made them attractive candidates. Unfortunately, the system did not exhibit enhanced lubrication properties. It is now believed that the small size of the C_{60} molecules was actually detrimental to its ability to reduce friction; instead of rolling over the surface, the C_{60} molecules would get trapped in surface asperities. Other nanometer-sized particle candidates that have been studied as potential lubricants include carbon nanotubes,[14−16] rod-shaped ZnS,[17,18] carbon nanopearls,[19] carbon nano-onions[20] and fullerene-like nanoparticles including WS_2 and MoS_2.[21−24] Recently, Vilt et al.[25] demonstrated the frictional performance of dry silica microspheres and showed direct evidence of the rolling behavior of spherical particles when sheared in confinement.

In this communication, we show that an aqueous colloidal suspension of uniform carbon microspheres ($C_{\mu sphere}$),[26] at concentrations as low as 0.1 wt %, stabilized by sodium dodecylsulfate (SDS) exhibits very promising lubrication properties. The sizes of the $C_{\mu sphere}$ particles used in this study (>400 nm) are sufficiently larger than the roughness of the shearing surfaces allowing them to easily roll over surface defects. Also, similar $C_{\mu sphere}$ particles have been shown to have a low degree of graphitization,[27,28] suggesting the presence of amorphous carbon (determined from X-ray diffraction), and therefore do not expose sharp surface facets (like crystals), which could potentially damage the shearing surfaces and impede efficient rolling. In addition, $C_{\mu sphere}$ particles have been demonstrated to withstand high pressures, on the order of 8 GPa,[29] before fracture. The size range, ease of synthesis, high monodispersity, and large yield stress of the $C_{\mu sphere}$, as well as the minimal environmental impact and low-cost of an aqueous-based formulation, are all desirable characteristics for the use of a $C_{\mu sphere}$-SDS suspension as an alternative lubricant to oil-based lubricants in compatible devices and machinery.

Uniform 450 ± 20 nm carbon microspheres (Figure 1a) were synthesized as described in the Experimental Section, following a protocol developed by Wang et al.[30] SDS was used to disperse the particles in water, as the final pyrolysis step in the synthesis

Received: May 10, 2011
Accepted: June 23, 2011
Published: June 23, 2011

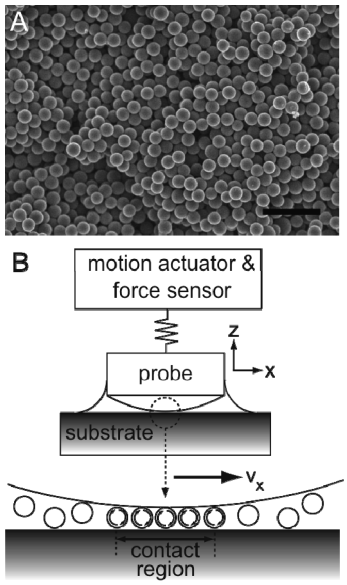

Figure 1. (a) SEM image of uniform 450 ± 20 nm carbon microspheres. The scale bar is 2 μm. (b) Schematic illustration of the (i) universal materials tester used to measure the friction force between two shearing surfaces and (ii) magnified view within the contact region.

renders the particles hydrophobic. Typical concentrations of the carbon particles used were approximately 1 mg mL^{-1} (0.1 wt % or 1 × 10^{10} particles mL^{-1}) while the SDS concentration was varied from the millimolar to molar range. A commercial universal materials tester (UMT) was used to measure the friction force and lubrication properties of the aqueous C$_{\mu sphere}$-SDS suspension between different flat surfaces and either a spherical silica or steel probe. A schematic of the instrument is shown in Figure 1b. The probe is attached to a sensor through a cantilever, and movement in the x and z direction is controlled by a motion actuator. A typical measurement consisted of applying an initial preload, shearing the surfaces at a fixed velocity v_x and distance, increasing the normal load, and repeating the shear cycle. The data was collected and analyzed digitally. A magnified view of the confined region in Figure 1b illustrates the lubrication mechanism of the C$_{\mu sphere}$. The motion of the top surface causes the particles in the contact region to roll, while the confined region is continuously replenished with C$_{\mu sphere}$ from the surrounding medium.

Figure 2 shows a plot of the friction force $\mathbf{F}_x$ between two shearing silica surfaces as a function of the normal load **L**. As a control, two silica surfaces were first sheared in the absence of any lubricant, resulting in a friction coefficient μ = 0.57. A second control experiment consisting of the same surfaces, with the addition of an aqueous SDS solution was performed to determine the lubricating contribution of the surfactant itself. In the presence of the aqueous SDS solution (0.36 M), the friction coefficient between two silica surfaces drops to 0.15 at high loads ($\mathbf{F}_z$ > 100 mN). At low loads, the friction force is similar to that obtained for shearing two glass surfaces without any lubricant. We attribute the lower friction coefficient with aqueous SDS as being due to the boundary lubrication provided by the SDS molecules preventing the silica surfaces from achieving true contact and being continuously replaced in the contact region. An aqueous C$_{\mu sphere}$-SDS suspension (0.36 M SDS, 1 mg mL^{-1} C$_{\mu sphere}$) provides the best lubrication with a friction coefficient μ = 0.03. The system fully follows Amontons' law, for load-controlled friction:[31,32] $\mathbf{F}_x = \mu\mathbf{L}$.

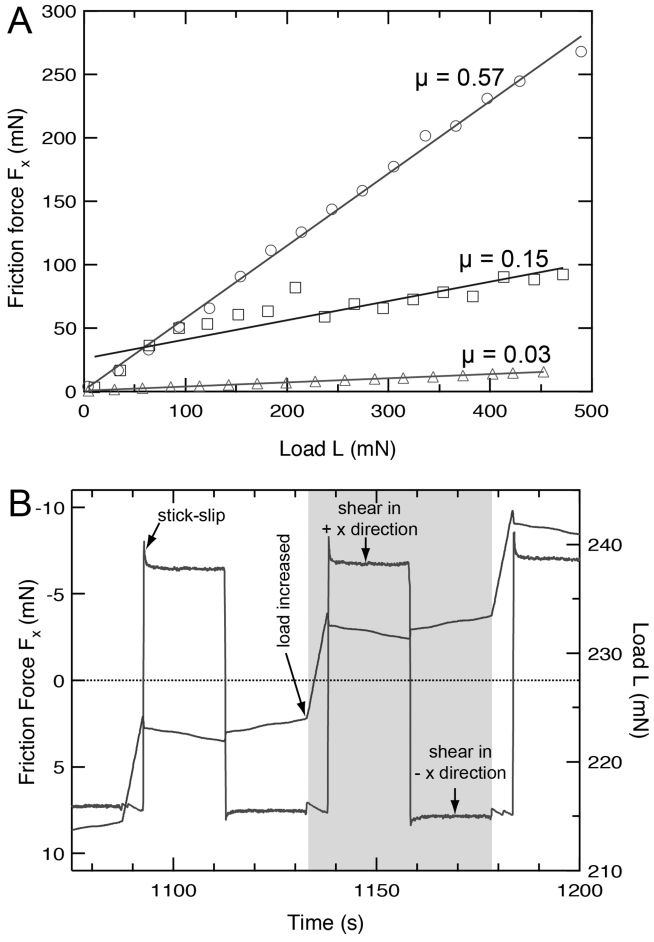

Figure 2. (a) Plot of friction force $\mathbf{F}_x$ versus applied load **L** while shearing a spherical silica probe versus a flat silica surface using (i) no lubricant (circle data point), (ii) an aqueous 0.36 M SDS solution as a lubricant (square data points), and (iii) an aqueous 1 mg mL^{-1} C$_{\mu sphere}$-SDS suspension as a lubricant (triangle data points). (b) Plot of a typical friction force $\mathbf{F}_x$ and applied load **L** trace versus time while shearing a flat silica probe versus a silicon surface in the presence of an aqueous 1 mg mL^{-1} C$_{\mu sphere}$-SDS suspension as a lubricant. The highlighted region corresponds to one shear cycle which starts with an increase in the load, followed by shearing in the $+x$ direction and ends with a shear in the $-x$ direction.

Similar μ values (0.03−0.04) are obtained with lower SDS concentrations, as low as 18 mM. Friction experiments were also performed with unmodified dry 800 nm C$_{\mu sphere}$ particles (without an aqueous medium). The latter also offer a low friction coefficient (μ = 0.06, see the Supporting Information Figure S1) when confined between two flat surfaces, but in the absence of SDS to stabilize the dispersion (see the Supporting Information for dispersion stability, Figure S2), lack the ability to migrate into and replenish the confined region in the event that the two shearing surfaces come into direct contact (e.g., when one of the shearing surfaces has a small radius of curvature). A segment of a typical friction and load trace between two silica surfaces, in the presence of the aqueous C$_{\mu sphere}$-SDS suspension, is shown in Figure 2b. The highlighted region corresponds to one shear cycle which includes an increase in the applied load **L**, followed by shearing in the $+x$ direction and ending with shearing in the $-x$ direction. After the load is increased, it remains virtually constant with a slight drift due to minor misalignments or a tilt in the

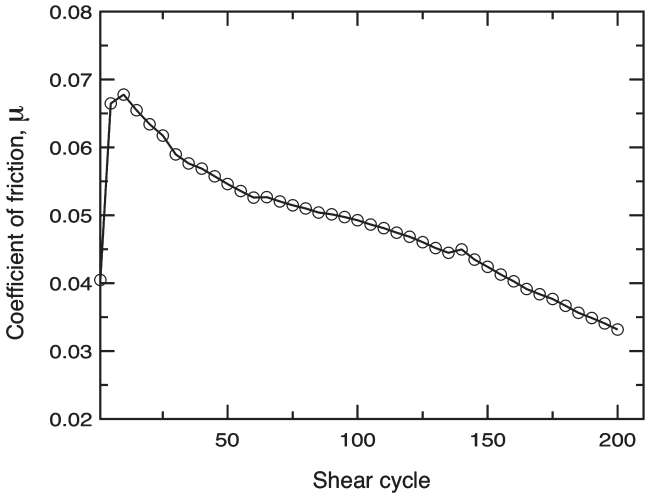

Figure 3. Plot of the coefficient of friction μ versus shear cycle for an extended run at a fixed load of 2.94 N using a spherical silica probe sheared against a silicon surface, with an aqueous 6.67 mg mL^{-1} $C_{\mu sphere}$-SDS suspension as the lubricant.

bottom silicon surface, which is experimentally unavoidable. Stiction spikes (or a single stick−slip event) in the force trace are prevalent at the beginning of the shear in the $+x$ direction followed by a smooth sliding motion. The spikes occur less frequently (either entirely absent or of smaller magnitude) at the beginning of the shear in the $-x$ direction, and are absent in experiments in which the load is kept constant between shear cycles, suggesting that the incremental load steps are responsible for the stiction spikes. The incremental load step can potentially squeeze out the particles from the confined region, thereby initially generating a high friction. The friction decreases to the point of smooth sliding only as the surface moves and the confined region is replenished with $C_{\mu sphere}$ particles.

The coefficient of friction between a silica bead and a silicon surface lubricated by a $C_{\mu sphere}$-SDS suspension was monitored for a long run of 200 shear cycles (total shear distance = 0.8 m) at a relative high constant normal load **L** = 2.94 N (Figure 3). The coefficient of friction is initially low but rapidly rises (within ~10 shear cycles) to a maximum. The latter is presumably caused by the jamming[33,34] of $C_{\mu sphere}$ particles in the confined region as a result of applying an initial high load, thus preventing efficient rolling. The coefficient of friction then gradually decreases over the duration of the experiment as layers of particles are squeezed out (or plowed away). Eventually a single layer of particles is expected to provide the lubrication. The experiment was terminated after 200 cycles because of the evaporation of the $C_{\mu sphere}$-SDS suspension, but future studies will include longer runs to determine at what point the coefficient of friction will finally level off. The pressure within the confined region is estimated to be between 100 and 400 MPa, based on the area of the contact region between the spherical probe and flat silicon wafer. Optical and SEM images of the sheared region, after the experiments were completed, show that the $C_{\mu sphere}$ particles remain intact, consistent with the fact that the pressures applied in these experiments were 1 order of magnitude below the yield stress of the $C_{\mu sphere}$ particles. Additional high-resolution characterization would be required to detect potential physical and chemical changes.

The effectiveness of a lubricant is not only measured by its ability to provide a low coefficient of friction but also by its ability

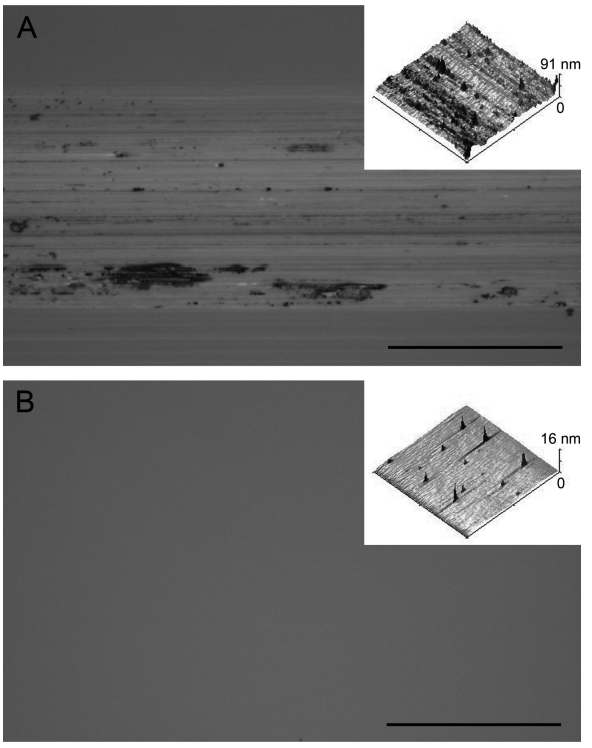

Figure 4. Optical image of the wear pattern formed after shearing a steel probe against a silicon surface at 441 mN (45 g) load for 10 cycles in the presence of (a) an aqueous 36.7 mM SDS solution as the lubricant, (b) an aqueous 6.67 mg mL^{-1} $C_{\mu sphere}$-SDS suspension as the lubricant. The scale bar is 50 μm. The insets are AFM images (30 μm × 30 μm) of the silicon surface within the wear pattern.

to reduce surface wear. Optical images of the wear pattern were captured after shearing a steel probe against a silicon surface, in the presence of an aqueous 36.7 mM SDS solution (Figure 4a), and an aqueous 6.67 mg/mL $C_{\mu sphere}$-SDS suspension (Figure 4b), as the lubricant for 10 shearing cycles at a constant load of 441 mN. In the absence of the $C_{\mu sphere}$ particles, surface damage occurs throughout the contact region and over the shear distance. The friction trace also shows stick−slip behavior with a relatively high friction coefficient μ = 0.3. In the presence of the $C_{\mu sphere}$ particles, surface wear is absent, as inferred from the optical image of the contact region. To further quantify the surface wear, AFM images were obtained within the wear patterns (insets of Figure 4). As expected, the surface damage is extensive (rms roughness = 7.2 nm) in the case in which only an aqueous SDS solution is used as a lubricant. Interestingly, no detectable surface wear was found when an aqueous $C_{\mu sphere}$-SDS suspension was used as a lubricant except for very sparse debris.

These results show that an aqueous $C_{\mu sphere}$-SDS (~0.1 wt %) suspension is an effective lubricant providing low friction coefficients on the order of 0.03, minimizing surface wear and avoiding degradation even at relatively high loads and prolonged durations. We propose that the lubricating properties of the $C_{\mu sphere}$ particles are a result of an efficient rolling mechanism and that these materials are of an appropriate size range to overcome getting trapped into surface asperities, and still be considered nano and microscale bearings. Continuing studies that seek to optimize the lubrication properties of these materials with biocompatible coatings could yield a new class of aqueous-based lubricants with potential applications to biolubrication.

EXPERIMENTAL SECTION

Friction Measurement. The experiments were performed with either smooth silica (rms = 1.72 nm, Anchor Optics, Barrington, NJ) or silicon surfaces (rms = 0.54 nm, test grade, University Wafer, Boston, MA) as the bottom shearing surfaces and either a curved silica surface (radius of curvature = 3 cm, Anchor Optics, Barrington, NJ) or a steel bead (Ø = 3.2 mm) as the probe (top surface). All surfaces were cleaned by sonication in ethanol for 5 min, followed by rinsing with water and a subsequent plasma-cleaning step (Harrick Plasma, Ithaca, NY). In a typical experiment, a drop (~50 μL) of the aqueous $C_{\mu sphere}$-SDS suspension (~1−10 mg mL^{-1} $C_{\mu sphere}$, 1 mM to 0.5 M SDS in water) was placed between the bottom surface and the probe, wetting both surfaces. Surface tension forces ensured that the aqueous suspension remained in the contact region. The probe, attached to a force sensor (FL, or DFM-0.5, CETR, Campbell, CA) with a cantilever (spring constant k_{FL} = 520 N/m, k_{DFM} = 4113 N/m), was then brought into contact with the bottom surface at a predetermined preload. A universal materials tester (CETR, Campbell, CA) was used to measure the friction force between the shearing surfaces as the load was either held constant or increased stepwise with each shear cycle. The coefficient of friction was determined by taking the slope of the average friction force versus the average load for each shear cycle. Longer runs, in which the evaporation of the aqueous-based lubricant was significant, were performed in a home-built enclosure with excess water in the surroundings to maintain high humidity.

ASSOCIATED CONTENT

Supporting Information. Additional figures and experimental details (PDF). This materials is available free of charge via the Internet at http://pubs.acs.org/.

AUTHOR INFORMATION

Corresponding Author
*E-mail: npesika@tulane.edu.

ACKNOWLEDGMENT

This work was supported by NSF Grant CBET-1034175. Additional funding was provided by the Advanced Materials Research Institute of the University of New Orleans through the PKFSI program. J.S. acknowledges a Graduate Fellowship from NASA and the Louisiana Board of Regents, BoRSF, under agreement NASA/LEQSF (2005−2010)-LaSPACE and NASA/LaSPACE

REFERENCES

(1) Mansot, J. L.; Bercion, Y.; Romana, L.; Martin, J. M. *Braz. J. Phys.* **2009**, *39*, 186–197.
(2) Tichy, J. A.; Meyer, D. M. *Int. J. Solids Struct.* **2000**, *37*, 391–400.
(3) Lin, T. W.; Modafe, A.; Shapiro, B.; Ghodssi, R. *IEEE Trans. Instrum. Meas.* **2004**, *53*, 839–846.
(4) Mang, T.; Dresel, W., *Lubricants and Lubrication*, 2nd ed.; Wiley-VCH: Weinheim, Germany, 2007.
(5) Kubo, K.; Kagaya, M.; Sunami, M.; Wakabayashi, T.; Watanabe, S. *Proc. Inst. Mech. Eng., Part J* **1999**, *213*, 1–12.
(6) Bartz, W. J. *Tribol. Int.* **1998**, *31*, 35–47.
(7) Blau, P. J.; Haberlin, C. E. *Thin Solid Films* **1992**, *219*, 129–134.
(8) Thundat, T.; Warmack, R. J.; Ding, D.; Compton, R. N. *Appl. Phys. Lett.* **1993**, *63*, 891–893.
(9) Bhushan, B.; Gupta, B. K. *J. Appl. Phys.* **1994**, *75*, 6156–6158.
(10) Schwarz, U. D.; Allers, W.; Gensterblum, G.; Pireaux, J. J.; Wiesendanger, R. *Phys. Rev. B* **1995**, *52*, 5967–5976.
(11) Schwarz, U. D.; Allers, W.; Gensterblum, G.; Wiesendanger, R. *Phys. Rev. B* **1995**, *52*, 14976–14984.
(12) Allers, W.; Schwarz, U. D.; Gensterblum, G.; Wiesendanger, R. *Z. Phys. B-Condens. Matter* **1995**, *99*, 1–2.
(13) Gupta, B. K.; Bhushan, B. *Lubr. Eng.* **1994**, *50*, 524–528.
(14) Cumings, J.; Zettl, A. *Science* **2000**, *289*, 602–604.
(15) Falvo, M. R.; Taylor, R. M.; Helser, A.; Chi, V.; Brooks, F. P.; Washburn, S.; Superfine, R. *Nature* **1999**, *397*, 236–238.
(16) Buldum, A.; Lu, J. P. *Phys. Rev. Lett.* **1999**, *83*, 5050–5053.
(17) Min, Y. J.; Akbulut, M.; Belman, N.; Golan, Y.; Zasadzinski, J.; Israelachvili, J. *Nano Lett.* **2008**, *8*, 246–252.
(18) Israelachvili, J.; Akbulut, M.; Belman, N.; Golan, Y. *Adv. Mater.* **2006**, *18*, 2589–+.
(19) Hunter, C. N.; Check, M. H.; Hager, C. H.; Voevodin, A. A. *Tribol. Lett.* **2008**, *30*, 169–176.
(20) Hirata, A.; Igarashi, M.; Kaito, T. *Tribol. Int.* **2004**, *37*, 899–905.
(21) Rapoport, L.; Bilik, Y.; Feldman, Y.; Homyonfer, M.; Cohen, S. R.; Tenne, R. *Nature* **1997**, *387*, 791–793.
(22) Rapoport, L.; Leshchinsky, V.; Lapsker, I.; Volovik, Y.; Nepomnyashchy, O.; Lvovsky, M.; Popovitz-Biro, R.; Feldman, Y.; Tenne, R. *Wear* **2003**, *255*, 785–793.
(23) Golan, Y.; Drummond, C.; Homyonfer, M.; Feldman, Y.; Tenne, R.; Israelachvili, J. *Adv. Mater.* **1999**, *11*, 934–+.
(24) Golan, Y.; Drummond, C.; Israelachvili, J.; Tenne, R. *Wear* **2000**, *245*, 190–195.
(25) Vilt, S. G.; Martin, N.; McCabe, C.; Jennings, G. K. *Tribol. Int.* **2011**, *44*, 180–186.
(26) Deshmukh, A. A.; Mhlanga, S. D.; Coville, N. J. *Mater. Sci. Eng., R* **2010**, *70*, 1–28.
(27) Wang, Q.; Li, H.; Chen, L. Q.; Huang, X. J. *Solid State Ionics* **2002**, *152*, 43–50.
(28) Zheng, M. T.; Liu, Y. L.; Xiao, Y.; Zhu, Y.; Guan, Q.; Yuan, D. S.; Zhang, J. X. *J. Phys. Chem. C* **2009**, *113*, 8455–8459.
(29) Pol, S. V.; Pol, V. G.; Sherman, D.; Gedanken, A. *Green Chem.* **2009**, *11*, 448–451.
(30) Wang, Q.; Li, H.; Chen, L. Q.; Huang, X. J. *Carbon* **2001**, *39*, 2211–2214.
(31) Amontons, G. *Mem. Acad. R. Sci.* **1699**, 206–222.
(32) Israelachvili, J., *Intermolecular and Surface Forces*, 2nd ed.; Academic Press: San Diego, 1992.
(33) Savel'ev, S.; Marchesoni, F.; Taloni, A.; Nori, F. *Phys. Rev. E* **2006**, 74.
(34) Desmond, K.; Franklin, S. V. *Phys. Rev. E* **2006**, 73.